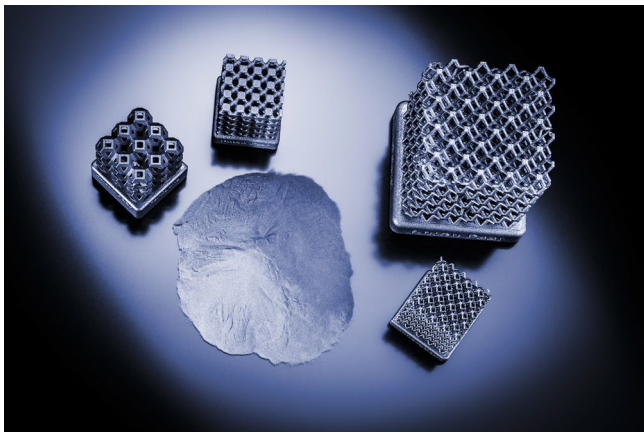


## Metal Powder Characterization

**Relevant for: powder rheology, metal powder, ceramic powders, selective laser sintering/melting, additive manufacturing, particle size analyzer, surface area, BET, true density, tap density**

Precision is paramount for making improvements in material design. In modern technology, metal powders are used in many different industries and for an extensive range of applications. This results in very diverse requirements due to the varied uses, e.g. additive manufacturing, casting, coating or additive in paints and inks, as well as a large range of industrial applications such as powder metallurgy, metal injection molding and toolmaking. Identifying powder properties is vital in order to know about physical properties. We investigate properties such as flowability, surface area, porosity, and size homogeneity, which affect the production process, as well as the final product quality.



### 1 Introduction

The microscopic properties of metal powders are of central importance in order to guarantee high quality of the raw as well as the final product. Typical powder analysis methods such as powder rheology, particle sizing, BET area and density measurements are, therefore, used for assessing the physical properties of these materials.

One typical application for the use of metal powders is 3D printing in the young field of additive manufacturing. Additive manufacturing processes, also known as layer construction processes, make it possible to create products of any size and complexity. This method is used in many industries including:

- consumer goods,
- medical technology,
- architecture, and
- aviation industry.

The heating chamber of the Anton Paar Convection Temperature Device 600 MDR is a model example for the need of additive manufacturing, even in series production. In contrast to conventional machining processes, the 3D printing technique allows for the formation of tightly formed hollow air channels within the 3D-printed shells. This guarantees homogeneous temperature distribution within the oven – with strong reduction of temperature gradients and minimized gas flow, resulting in reduced drying and air vortices.

The most common technique for metal 3D printing is selective laser melting. In this approach, a thin layer of metal powder is first placed on a flat surface. A high power laser beam is then guided across the plane and selectively melts the powder particles together where bulk metal is desired in the finished piece. Afterwards, another layer of powder is added and the laser maps the area again. Those two steps are repeated until a structure of bulk metal has formed, surrounded by remaining powder. Finally, the residual powder is removed to yield the final part. Since the possibility of applying a thin and homogeneous powder layer as well as melting the particles together with the laser is crucially dependent on the physical properties of the metal powder, knowledge of:

- flow properties,
- fluidizability,
- porosity,
- compressibility,
- cohesion strength or
- particle size distribution (PSD)

aid both the manufacturing process and the quality of final products.

As described before, the remaining powder is removed from the bulk work piece and can be reused. Although this is beneficial from an economic and environmental points of view, the change of physical properties with each production run has to be controlled in order to further ensure a smooth manufacturing process as well as final product quality and stability.

Metal powder particles used for selective laser sintering are typically in the range of 20 to 100  $\mu\text{m}$ . This size, together with the prerequisite of being spherical, enable good flow behavior when adding new powder layers. The laser power and scan rate have to be sufficient to introduce enough heat to the particles for the melting process. Finally, the macroscopic appearance of the product strongly depends on the particle size of the raw powder. Particles that are too large lead to a rough surface finish. A wide particle size distribution is also not desirable, since both the flow behavior in the powder state, as well as the microstructure of the finished product will suffer greatly.

Anton Paar offers a versatile toolbox for characterization of powders: Laser diffraction methods measure particle and aggregate sizes, powder rheology enables characterization of their flow and mechanical behavior, and surface area analyzers unite these methods with physical adsorption techniques.

Laser diffraction is the ideal technique for finding out the particle size distribution of powders in this size range. It enables fast and reliable measurements for deciding whether the present powder fulfills the required manufacturing criteria. The **Particle Size Analyzer (PSA)** allows powder dispersion in a liquid where agglomerates can be broken down by sonication, but also with compressed air in the Venturi in dry mode. Very coarse particles of up to 2.5 mm can be measured in the free-fall mode. With the robust design of the PSA and the easy to use software Kalliope, this instrument is ideal for quality control in metal powder production.

Powder rheology can characterize powders using two unique powder cells on rheometers: the **powder flow cell** and the **powder shear cell**. These two cells provide the means for comprehensive characterization of powder properties such as flow behavior, fluidizability, cohesion strength, permeability, compressibility, tensile strength and more. With these parameters, the powder behavior can be characterized under the conditions closely reflecting every step of the application. In the powder shear cell it is even possible to control the ambient conditions with a humidity range from 5 % RH to 95 % RH and an extensive temperature range from -160 °C to 600 °C.

One of the main barriers to widespread use of additive manufacturing technologies is the prohibitive cost of the metal powders. Any step for gauging suitability of any given material for reuse offers much potential to save running costs.

## 2 Powder Rheology

### 2.1 Challenges

When producing, storing or processing metal powders, a large variety of challenges can occur. With the two unique cells for powder rheology (powder flow cell and powder shear cell) any powder can be characterized in its applied state. The typical challenges that can be approached with the two powder cells are:

- flow properties, e.g. transport and raking by the 3D printing machine,
- reusability and recyclability,
- final product quality,
- silo discharge, and
- filling and dosing.

Powder characterization enables optimization of processing parameters, avoiding issues e.g. during raking. The results can also be used to find out how a powder changes during reuse and recycling. All this helps ensure optimized printing processes and precise products.

### 2.2 Materials and Experimental Setup

Selected measurements are shown on two different metal powders: stainless steel (1.4404) and silver. Both are used for additive manufacturing. The stainless steel samples were measured with the powder flow cell and the silver samples were measured with the powder shear cell. The powder flow cell is ideal for measuring free-flowing powders under very low loads or their own weight. The powder shear cell is better suited for cohesive powders (such as silver) under high loads, but the results can be extrapolated to lower loads.



Figure 1: Modular Compact Rheometers (MCRs) equipped with a powder flow cell (left) and a powder shear cell (right).

## 2.3 Measurement and Results Powder Rheology

### 2.3.1 Powder Flow Cell: Cohesion Strength

Cohesion strength describes the internal resistance of the powder to flow, and thereby is a measure of powder flowability. These measurements are fast with astounding reproducibility and are a helpful quality control tool for predicting powder behavior. The sensitivity and reproducibility of this method helps differentiate even very similar powders or tiny changes within individual powder batches. (1)

Stainless steel powders were measured with this method. The sensitivity is reflected in this measurement of the powders as received and in recycled state, with results displayed in Figure 2 and summarized in Table 1. The sample R00 is fresh metal powder, while the numbers on the other samples indicate how often they have been reused and recycled (with RXX for over 20 times reuse).

The measurements show an increase in cohesion strength with an increasing number of 3D printings. The structure of some of the particles changes after every process run, such as formation of irregularly shaped particles e.g. due to spattering. After every use the powder is sieved, which also causes slight changes in the particle size distribution of the powder. All these changes are reflected in the cohesion strength method. Other possible changes, which can cause a measurable structural change, include high-temperature effects, oxidation or melting and welding effects.

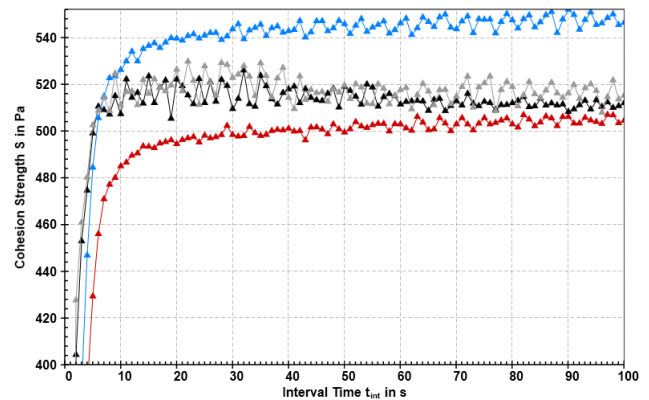


Figure 2: Cohesion strength of stainless steel powders: R00 (red), R01 (black), R05 (gray), RXX (blue).

Sample	Description	Cohesion Strength [Pa]
R00	Fresh powder	506.3
R01	Used once	512.7
R05	Used 5 times	522.2
RXX	Used > 20 times	551.5

Table 1: Cohesion strength of stainless steel powder from fresh (R00) to used (RXX) powder.

For raking (i.e. doctor blading or rolling, depending on the individual machine used) it is generally advisable to aim for a high flowability (and low cohesion) since high cohesiveness during these processes inevitably leads to a rough surface and, furthermore, imprecise parts.

The same measurement can not only be used for predicting flow behavior, but also provides information on the air-holding capacity. For this analysis an enlarged part of Figure 2 is displayed in Figure 3. Here, the sample R00 (red) shows the lowest incline and, therefore, the highest air-holding capacity. The slope steepens with the number of build-jobs, indicating a decreasing air-holding capacity.

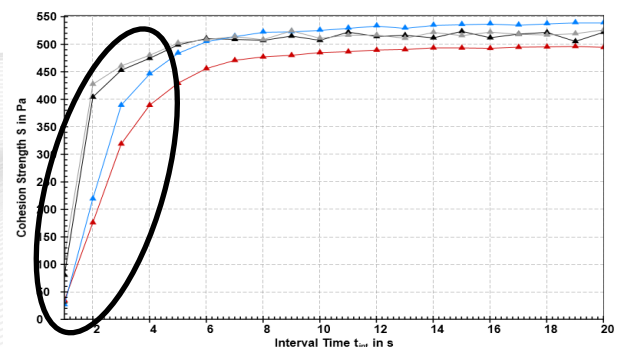


Figure 3: Illustration of different slopes in the beginning of cohesion strength measurements: R00 (red), R01 (black), R05 (gray), RXX (blue).



Further parameters, which can be analyzed with the powder flow cell include compressibility, permeability, wall friction, fluidization properties and many more. (1)

### 2.3.2 Powder Shear Cell: Flowability

Shear cell measurements are used for analyzing flow behavior as well as retrieving a wide range of other powder properties such as angle of internal friction, cohesion, unconfined yield strength and more. The powder shear cell can be used in combination with heating chambers and a humidity option, enabling precise temperature and humidity control.

The powder shear cell measurements shown here were carried out on silver powder used in additive manufacturing.

The measuring parameters were chosen with a pre-shear at a normal stress of 6 and 9 kPa, and five shear points per pre-shear normal stress. The yield locus curves from the shear measurements are displayed in Figure 4. These curves are a result of the measurements at different stress conditions and allow the analysis of powder parameters.

The shear cell can yield a large number of different parameters. This report focuses on cohesion, tensile strength, and unconfined yield strength. Cohesion  $\tau_c$  is the resistance of the powder to flow when stress is no longer applied to the powder and is a measure of flowability. The tensile strength  $\sigma_t$  is the pressure required to separate one layer of powder from another and is useful for simulation and quality control. Unconfined yield strength  $\sigma_c$  describes the “strength” of the powder and can be useful for tableting and silo design, while the major principle stress  $\sigma_1$  gives the total stress applied to the powder during the test (consisting of normal and shear stress). An overview of these parameters for the silver powders can be found in Table 2.

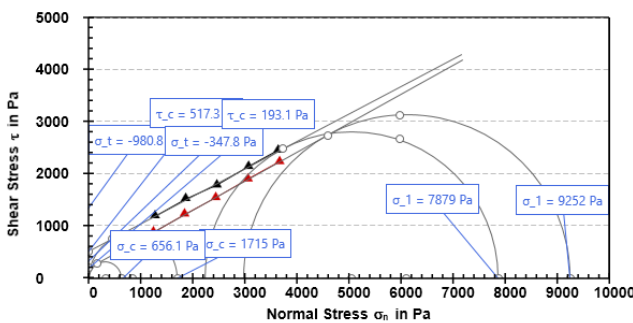


Figure 4: Yield locus curves of two silver powders, measured at 6 kPa compaction: Ag01 (red), Ag02 (black).

The unconfined yield strength  $\sigma_c$  of Ag01 is significantly lower than that of Ag02, meaning less stress and force is needed to move, rake and process Ag01. The cohesion  $\tau_c$ , as well as the tensile strength  $\sigma_t$  of Ag01 are much smaller than that of Ag02, indicating better flowability at low loads, as is the case during raking or doctor blading in additive manufacturing.

Parameter [Pa]	Ag01	Ag02
$\sigma_c$	656.1	1715.0
$\sigma_t$	347.8	980.8
$\tau_c$	193.1	517.3

Table 2: Powder parameters from the yield loci of two silver powders, measured at 6 kPa compaction.

The yield locus curves were also recorded at 3 kPa compaction and could then be used to analyze flowability (Figure 5) together with the 6 kPa measurements. Regarding flowability, the two samples show distinct behaviors, where Ag02 is easy-flowing, while Ag01 is transitioning from easy to free-flowing with increasing precompaction. Due to the construction of metal additive manufacturing machines using a deep shaft for storage and, therefore, applying various loads on the top of the powder during a complete run, it is highly desirable to have a powder that does not react strongly to precompaction. This is the case, as can be seen in Figure 5, since the flowability function of the two silver powders run nearly in parallel to the quadrant border.

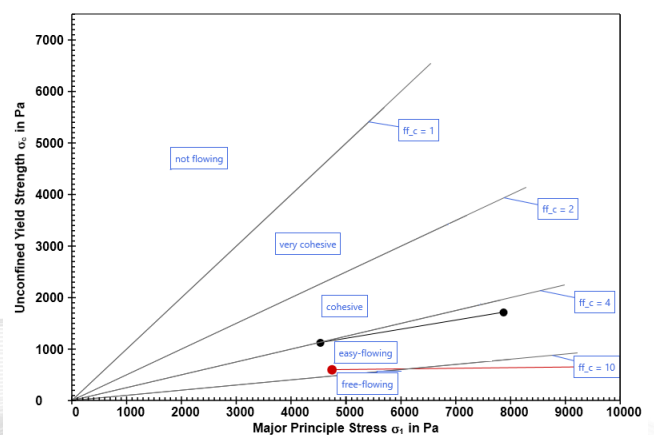


Figure 5: Flowability curves of two silver powders, measured at 3 and 6 kPa consolidation: Ag01 (red), Ag02 (black).

### 3 Particle Size Analysis

#### 3.1 Challenges for Particle Characterization

In the production of metal powders, laser diffraction is a widely used quality control technique, due to its reliability, simplicity and the compatible size range of the materials used.

To produce an optimal raw powder, trade-offs have to be made. Very fine particles with narrow size distributions are prone to agglomeration, while segregation occurs with large particles and broad particle size distributions. (2) With the PSA, particle size distributions over all ranges of interest can be studied.

#### 3.2 Materials and Experimental Setup for Particle Characterization

Two different production batches (Batch 1, Batch 2) of fresh (i.e. R00) stainless steel powders used for laser sintering (1.4404, as above) were measured with the PSA 1190 LD in liquid mode. The dispersion medium was water. In order to stabilize the dispersion and avoid agglomeration of the fine fraction, sodium metaphosphate (NaMP) was added to the water tank to achieve a 1 g/L concentration. To ensure a representative sample, the batch was slowly rotated by 360°, then the sample was taken from a sideways position. Stainless steel powder was added to the water tank, until a stable obscuration of approximately 10 % was achieved. The stirrer was set to full speed, in order to keep the dense particles dispersed. As the optical properties of the sample are known, the Mie model was used for analysis. The input parameters are summarized in Table 3.

Parameter	Value
Sample dispersion	1 min
Measurement time	30 sec
Ultrasound	50 W
Stirrer	450 rpm
Pump speed	120 rpm
Reconstruction model	Mie
Refractive index (635 nm)	2.9 - 3.4i (3)
Refractive index (830 nm)	2.9 - 3.1i (3)
Repetitions	3

Table 3: Input parameters for the measurement of stainless steel.

### 3.3 Results and Discussion

#### 3.3.1 Particle Size Distribution of Metal Powders

Figure 6 shows the particle size distribution of two batches of stainless steel powder.

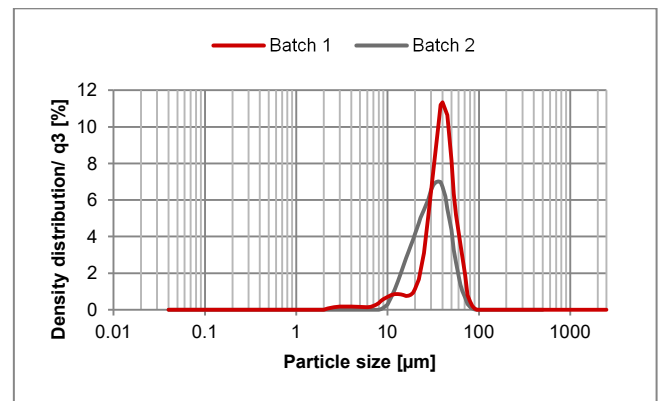


Figure 6: Particle size distribution of two different R00 batches of the same stainless steel powder.

The results of both powders show a main peak at around 40 µm, which is one of the specifications of the product. Furthermore, both batches have a very clear maximum particle size of around 90 µm. However, a clear discrepancy can be observed in the lower size range. While Batch 1 shows two additional side peaks at 10 and 4 µm, Batch 2 reflects a single, broader peak spanning from 10 to 90 µm. This difference is also reflected in the volume-based undersize D-values, summarized in Table 4.

Sample	D <sub>10</sub> [µm]	D <sub>50</sub> [µm]	D <sub>90</sub> [µm]
Batch 1	19.1	36.7	54.3
Batch 2	15.4	29.0	48.2

Table 4: Volume-based undersize D-values of stainless steel powders (average of three measurements).

The presence or lack of a fine fraction has a significant effect on the properties of powders (e.g. flow properties and segregation), and therefore, also on the sintering process and the end product.

In order to investigate the small particles present in Batch 1 but not in Batch 2 in more detail, the sample was first sieved with a 30  $\mu\text{m}$  mesh sieve (Batch 1\_Sieved). This sieved sample was furthermore dispersed in 1 g/L NaMP solution, ultrasonicated for 10 min, and subsequently left to sediment for 1 min. The resulting aqueous phase was still turbid due to the fine fraction sedimenting slower than the coarse particles. With the coarse particles already settled to the bottom, the remaining liquid phase was pipetted into the water tank of the PSA and measured (Batch 1\_Fine fraction). Figure 7 displays the particle size distribution of Batch 1 from stock and after the two steps to extract the fine fraction. As can be seen, the whole particle size range was already well represented while measuring the stock sample. The onset of the particles contributing considerably to the PSD by volume starts at a diameter of approximately 2  $\mu\text{m}$ . With the segregation method, this fine fraction (2 – 11  $\mu\text{m}$ ) could be extracted efficiently.

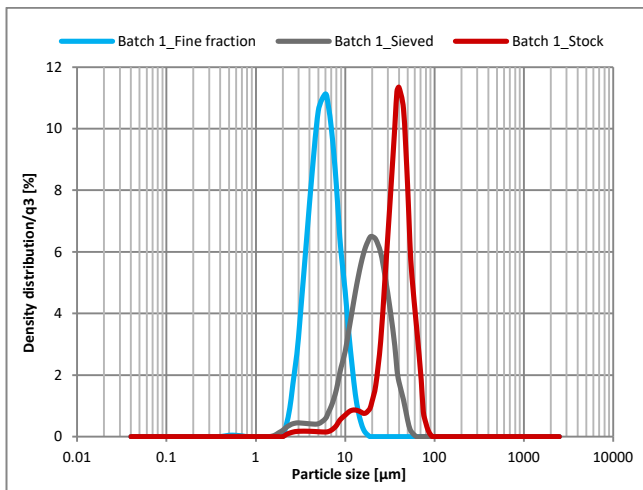


Figure 7: Particle size distribution of different fractions of fresh stainless steel powder from Batch 1.

It is worth noting, that the 30  $\mu\text{m}$  mesh-sieved sample also clearly shows a population of particles in the size range of 30 - 60  $\mu\text{m}$ . This might be surprising at first glance, but happens due to the well-known fact, that sieving selects the particles according to their smallest dimension. In the microscope picture of the sieved sample (Figure 8), the presence of elongated particles with lengths of 40 - 60  $\mu\text{m}$  and a width of about 30  $\mu\text{m}$  confirms this. Since there are only two or three of these particles visible in the picture, these might be considered negligible. In contrast, the PSD clearly shows that the few particles, which have twice the volume of a single spherical particle, are responsible for a significant volume fraction of the sieved sample. Hence, the clear relevance of laser diffraction for monitoring the real particle size, also after a sieving process, is proven.

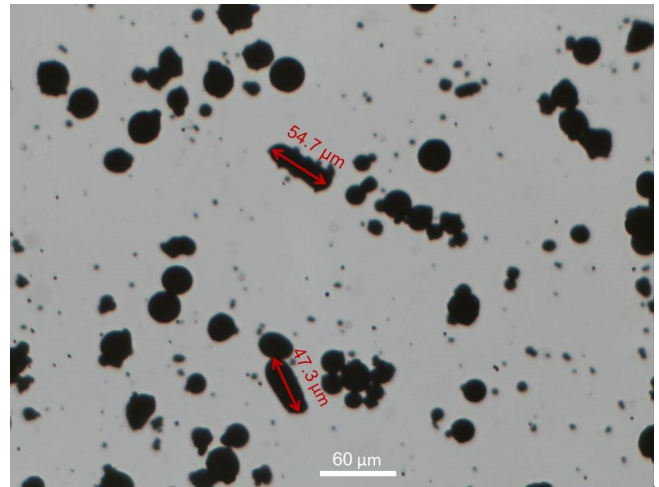


Figure 8: Microscope image of Batch 1\_Sieved. Indicated with red arrows are two elongated particles, which clearly exceed 30  $\mu\text{m}$  in one dimension.

## 4 Powder Density and Specific Surface Area

### 4.1 Challenges for Powder Density and Specific Surface Area Characterization

Characterizing a metal powder's specific surface area and density characteristics are often used quality control measures. In fact, ASTM methods have been developed for characterization of metal powders. In this section, we tested specific surface area per ASTM B922, tap density per ASTM B527, and skeletal density per ASTM B923. These properties help determine the metal powder's consistency from batch to batch, which can affect the following downstream properties:

- sintering behavior,
- dispersion,
- chemical composition,
- flowability and powder packing, and
- agglomeration.



## 4.2 Materials and Experimental Setup for Powder Density and Specific Surface Area Characterization

### 4.2.1 True and Tapped Density

The stainless steel powder metal samples (as used for powder rheology and particle size analysis) for tapped density and true density measurements were used as received. Additionally, aluminum (Al) powders were analyzed. The powders were shaken in a closed container prior to adding them to the sample chamber using a transfer funnel to a graduated cylinder. Using an Anton Paar Dual Autotap, the cylinder was lifted and dropped from a 3.0 mm height for each tap. An Anton Paar micro pycnometer was used for true-density measurements, approximately three-fourths of the large micro sample cell volume (~7 g stainless steel or ~2 g Al) was filled and the sample was purged with He for one minute prior to density measurements using He for analysis.

### 4.2.2 BET Surface Area

The powder metal samples for BET (Brunauer-Emmett-Teller) surface area measurements were prepared by applying vacuum to the sample at 150 °C for two hours prior to measurement. A nitrogen adsorption experiment was performed using Anton Paar's NOVAtouch vacuum volumetric gas adsorption analyzer at the relative pressure range from 0.05 to 0.3 ( $P/P_0$ ), for which a linear plot of  $1/[W(P_0/P)-1]$  vs.  $P/P_0$  was used to apply the BET equation and determine the accessible surface area.

Note: the slope, intercept and BET C constant values must always be positive.

## 4.3 Measurement and Results for Powder Density and Specific Surface Area Characterization

### 4.3.1 True and Tapped Density

The initial true He density for the stainless steel powder was 7.8373 g/cm<sup>3</sup> (R00), which did not change significantly upon multiple recycling to 7.8713 g/cm<sup>3</sup> for RXX. Similarly, the He density measurements for the Al samples were 2.6474 and 2.6294 g/cm<sup>3</sup> for R00 and RXX, respectively. However, the tapped densities decreased from 5.33 to 5.20 g/cm<sup>3</sup> for stainless steel and from 1.74 to 1.70 g/cm<sup>3</sup> for aluminum. This decrease in packing densities can be used together with the cohesion strength data to reveal that physical changes to the bulk particle size occurred upon recycling.

### 4.3.2 BET Surface Area

The calculated BET accessible surface area values for the experimental nitrogen adsorption isotherm (Figure 9, BET plot) were 0.37 and 0.46 m<sup>2</sup>/g for stainless steel R00 and RXX, respectively. This slight change may be caused by either a physical change to the spent material, with increased surface roughness, or a chemical change, such as surface oxidation. These surface area values are consistent with similar materials of their size domain.

The BET areas for Al were 1.19 and 1.22 m<sup>2</sup>/g for R00 and RXX, respectively. This minor change in surface area of ~3 % could shed light on the 20 % difference for the spent stainless steel as the Al particles would not further oxidize.

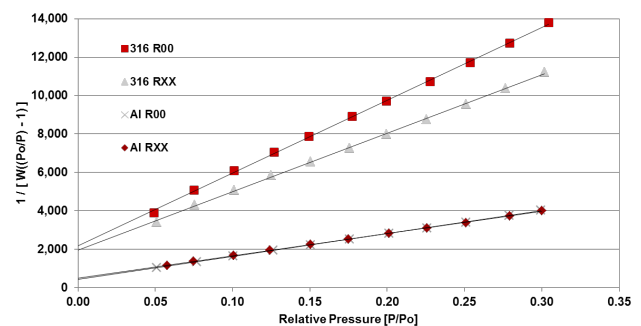


Figure 9: BET plots at 77 K for 316 R00 (red square), over 20-time usage RXX (gray triangles), new Al R00 (gray X) and over 20-time usage Al RXX (red diamond), all with their line of best fit for BET area calculation.

## 5 Conclusion

The challenges in regard to manufacturing, handling, and processing metal powders can be addressed by the techniques and instruments introduced in this report. As shown with the example of metal powders for selective laser sintering used in the field of additive manufacturing, a wide variety of properties can be investigated. The flow behavior, for instance, is governed by a multitude of aspects such as particle size, size distribution, morphology. Understanding the flow properties via powder rheology helps predict the powder behavior during processing and storage. This can, for example, be used to predict how a powder will behave in the process, but also to analyze the degree to which it is recyclable. Ideally a powder should be as free-flowing as possible, have low tensile strength and angle of internal friction and react as little as possible to applied normal stress. For both types of analyzed powders, this was the case.

The particle size distribution of the raw powder strongly influences the manufacturing process itself as well as the quality of the final work piece. For instance, very fine particles with narrow size distributions are prone to agglomeration, while segregation occurs with large particles and broad particle size distributions. Although two production batches from the same manufacturer's powder were investigated, significant differences were found by analyzing the particle size distribution with the PSA. As could be shown, sieving doesn't cause the expected narrowing of the PSD, since elongated particles of twice the mesh size are able to pass, causing a significant volume fraction of particles being bigger than the sieve mesh.

The differences occurring from the starting powder particles to the recycled powder particles can cause manufacturing and product issues. With the techniques used here, standards can be developed to alleviate these issues.

In conclusion, the wide range of analysis techniques to assure suitability of powders for additive manufacturing processes were demonstrated in this report. These can either be used as entry control or to gauge the powder's suitability after recycling.

## 6 References

1. **Anton Paar GmbH**. *Introduction to Powder Rheology*. Application Report. D43IA011EN-C.
2. *The role of particle size on the laser sintering of iron powder*. **Simchi, A.** 5, s.l. : Springer-Verlag, Oct 1, 2004, Vol. 35, pp. 937-948. 1543-1916.
3. *Optical constants of transition metals: Ti, v, cr, mn, fe, co, ni, and pd*. **Johnson, P.B. and Christy, R.W.** 12, s.l. : APS, 1974, Physical review B, Vol. 9, p. 5056.

### Contact Anton Paar GmbH

Tel: +43 316 257-0  
rheo-application@anton-paar.com  
application-sp@anton-paar.com  
pc-application@anton-paar.com  
www.anton-paar.com